



www.editada.org

Shannon Entropy in the Automatic Identification of Microbleeds Using Image Processing

Alina Villanueva¹, Rafael Guzman-Cabrera^{2,*}, Aron Hernandez-Trinidad^{1,*}, José Soto¹, Teodoro Cordova-Fraga¹

¹ División de Ciencias e Ingenierías, Universidad de Guanajuato campus León, GTO, México.

² División de Ingenierías, Universidad de Guanajuato campus Irapuato-Salamanca, GTO, México.

*E-mails: guzmanc@ugto.mx, aron.hernandez@ugto.mx

Abstract. The detection of microbleeds in Magnetic Resonance Imaging (MRI) studies through the Susceptibility Weighted Image (SWI) technique is presented. The SWI technique has shown to play a relevant role in the identification of microbleeds, unlike conventional MRI techniques, the sensitivity is higher for detecting microbleeds and iron deposits. This work presents a technique for the quantitative detection of microbleeds through the implementation of Shannon entropy. It is complemented with a statistical analysis of the results and establishes a specific range that allows for the early detection of these structures in future research. Preliminary results suggest that this method represents a significant advancement in the accurate and timely detection of cerebral microbleeds, offering an alternative to traditional Magnetic Resonance approaches, suggesting that artificial intelligence is a promising path for deeper investigations in this field.

Keywords: SWI, Microbleeds, Shannon Entropy.

Article Info

Received Dec 26, 2016

Accepted Dec 11, 2017

1 Introduction

It is known that the Susceptibility Weighted Image (SWI) technique is useful in the diagnosis of neurodegenerative diseases such as Alzheimer's, Parkinson's disease, multiple sclerosis, and neuromuscular diseases. These pathologies generally involve the formation of microbleeds, which are directly related to progressive cognitive decline [1]. Cerebral microhemorrhages are tiny deposits of hemosiderin, which can manifest in Magnetic Resonance Imaging (MRI) or computed tomography (CT) images of the brain as hypointense areas. They tend to appear oval or circular with a diameter of 5 to 10 mm. These microhemorrhages are indicators of various brain disorders [2]. The detection of microhemorrhages presents a challenge in the diagnostic process due to their morphology and variability in size, which tends to increase with the progression of neurodegenerative disease [3]. The lack of sufficient contrast in the images makes microbleed detection difficult. Despite being a useful tool for detecting such pathologies, computed tomography presents the problem of not distinguishing between calcifications, veins, and microhemorrhages and even being prone to the "blooming" effect [1,3]. The SWI technique, with its image processing, provides susceptibility and high contrast in microhemorrhages compared to other techniques such as T2* and GRE, especially when performed at 1.5 Tesla [4]. SWI has higher sensitivity to these brain anomalies that cannot be detected by conventional MRI [5,6]. The detection of microbleeds depends on various parameters, which allow them to be classified based on size, intensity, location (usually in the white matter) [7], distribution, resolution, signal-to-noise ratio, echo time (TE), field strength, and susceptibility [8].

There are various techniques for the detection of microbleeds, ranging from classic methods such as thresholding, seed growing, among others, to slightly more advanced techniques based on specific patterns such as Fast Radial Symmetry Transform in 3D [9], methods that automatically segment images where each segment presents a probability of detecting certain objects (YOLO) [10], and even techniques that combine previous methods to classify the anomaly of interest more accurately (Bayesian classifiers) [11]. Currently, there are semi-automatic and automatic methods for the segmentation and detection of these microbleeds, which propose various techniques aimed at reducing detection time [12]. The use of neural networks allows for precise and automatic detection to improve classification capability [13], aiming to avoid manual detection, which tends to have errors, although they

are prone to false positives [14]. One of the main advantages of some algorithms is their quantitative approach, which allows us to rely on pure image information, thus avoiding false detection by the observer or even the expert [15].

In the present study, a technique is proposed for the detection of microbleeds using Shannon entropy in digital image processing. Entropy quantifies the amount of information in an image by measuring the uncertainty or randomness in its values. A higher entropy value indicates more information and thus better image quality. The entropy mentioned here is Shannon entropy, which is defined in terms of the probability of occurrence of pixel values in the original image. It is used to measure uncertainty in the information source and is expressed in terms of the number of gray levels present in the image [16].

The technique has been previously employed in various investigations focused on digital image processing for edge detection, such as object contours, obtaining a grayscale threshold automatically using the firefly method [17, 18]. Shannon entropy has also been utilized for edge detection using methods such as Baljit, Amar, Renyi, among others [19, 24], proposing a new measure of image randomness in the absence of patterns through block division [25], and even in image understanding based on creating multi-level images using Shannon entropy and differential evolution [26, 27]. In different studies, entropy-based methods have been proposed for various applications, such as multiple sclerosis identification and anomaly detection in mammography, tumor detection, cell identification, and subsequent reconstruction [16].

So far, there is no record of its application in the detection of cerebral microbleeds, especially with the specific method [28] that we are employing to address this issue.

Following, in Section 2, the materials and methods employed in conducting this study are detailed, including a description of the database used and a more detailed explanation of the concept of Shannon entropy. In Section 3, the proposed method for microbleed detection is presented, along with an explanation of the algorithm used. Subsequently, in Section 4, the results obtained are analyzed, including a brief statistical analysis and interpretation of the findings. Finally, in the last section, the conclusions of the study are presented, and relevant acknowledgments are expressed.

2 Materials and Methods

The dataset used in this work consists of 57 MRI SWI scans from 30 patients with cerebral microbleeds, in addition to 100 healthy patients with 313 scans. The Shannon entropy method is intended to be used for the detection of cerebral microbleeds.

2.1 IRM Dataset

The dataset was published on May 11, 2021, under the name "Biomedical Informatics Group ResDevCons" by the Biomedical Informatics Group, led by Jurgen Mejan-Fripp, as part of the organization CSIRO (Australia), Austin Health, Heidelberg (Australia) [29]. The images are of the NIFTI-GZ type, with dimensions of 165.00x240.00 mm (176x256); 32-bit, 14MB.

2.2 Shannon Entropy

Shannon entropy is a fundamental concept in information theory and probability, introduced by Claude Shannon in 1948. In general terms, it is used to quantify the uncertainty or degree of disorder present in a dataset or information system.

In the realm of information theory, Shannon entropy is defined as the average measure of the information contained in a dataset, expressed in terms of the probabilities of occurrence of different outcomes. The higher the entropy, the greater the uncertainty in the data. Conversely, low entropy indicates that the data is more predictable. Mathematically, Shannon entropy, denoted as $H(x)$ for a discrete variable X with n possible outcomes, is calculated using the formula:

$$H(X) = - \sum_{i=1}^n P(x_i) \cdot \log_2(P(x_i)) \quad (1)$$

Where $P(x_i)$ represents the probability of outcome x_i occurring.

Shannon entropy can also be interpreted as the minimum average amount of bits required to represent the information contained in the random variable X . When the data is completely predictable (i.e., when the probability of one outcome is 1 and all others

are 0), the entropy is zero, indicating the absence of uncertainty and the lack of need for additional information to describe the data [29,30].

Shannon entropy has various applications in fields such as communication theory, data encoding, file compression, cryptography, image processing, among others. In the context of image processing, Shannon entropy is used to characterize the distribution of pixel intensities in an image and provide information about its content. One application is texture analysis, where entropy is used to quantify the variability or irregularity in the distribution of pixel intensities within image regions representing textures. The higher the entropy, the greater the variability in textures, which may indicate greater complexity or information in the image. This entropy is also used in image segmentation to divide an image into meaningful regions or classes based on the variability of pixel intensities [31-34].

2.3 Proposed Method for Microbleed Detection

To microbleeds in MRI images, an algorithm utilizing Shannon entropy is applied. This is because of its beneficial nature in image processing, as it provides a quantitative measure of the information contained in an image, which is useful for assessing the complexity and information content of an image. The method presented in this work aims to detect cerebral microbleeds in a unique way, unlike previous approaches. This method allows for quantitative detection rather than qualitative detection, as traditionally done. Previous methods often rely on patterns, shapes, positions, intensities, among others, which can make them susceptible to errors during evaluation. When dealing with patients, precision is crucial, with minimal margin for error. Therefore, considering even the possibility of error elimination with the assistance of artificial intelligence is essential.

The proposed method consists of the following general steps:

1. Define a function to calculate the entropy of the 50 images from healthy patients.
2. Divide each image into sections and calculate the entropy for each section.
3. Calculate the means and standard deviations per section.
4. Load a new image for analysis where the patient has microbleeds.
5. Divide the new image into sections and calculate the entropy for each section, repeating steps 2 and 3 but for the new image.
6. Compare the entropies of the new image with the means and standard deviations.

Algorithm 1: General framework of the proposed method using healthy images

Input: 50 images of cerebral microbleeds with healthy patients

Output: Obtaining segmented images averaged based on Shannon entropy

1. Normalize the histogram of the images
 2. *def* Calculation of Shannon entropy for each image section
 return images entropy
 3. *for* iteration over each image
 | *if not* directory not found
 | image dimensions
 | divide image into predefined sections
 | *for* calculate entropy for each part of the image
 4. *for* Calculate means and standart deviations per section
-

Fig. 1. Algorithm used in phase one showing the process carried out with images of healthy patients.

Algorithm 2: General framework of the proposed method using microbleed images

Input: New image to analyze

Output: image with divisions along with their respective Shannon entropy compared to healthy images, detecting if there is microbleeding

1. *If* the directory is correct
 else image dimensions
 segment the image
 2. *def* calculation of Shannon entropy for each section of the image
 | *for* i in image dimensions
 return images entropy for each section
 3. *for* calculate the means and standart deviations per sections
 4. *for* compare the entropies of the new image with the means and standart deviations
-

Fig. 2. Algorithm used in phase two showing the process carried out with images of patients with microbleeds.

The first phase involved selecting 50 images of healthy patients for processing using an algorithm specifically designed for obtaining entropy. The sample size was chosen according to the central limit theorem, as shown in Fig. 3. Each image was divided into 16 equal sections, allowing for a detailed examination of different areas, as illustrated in Fig. 4.

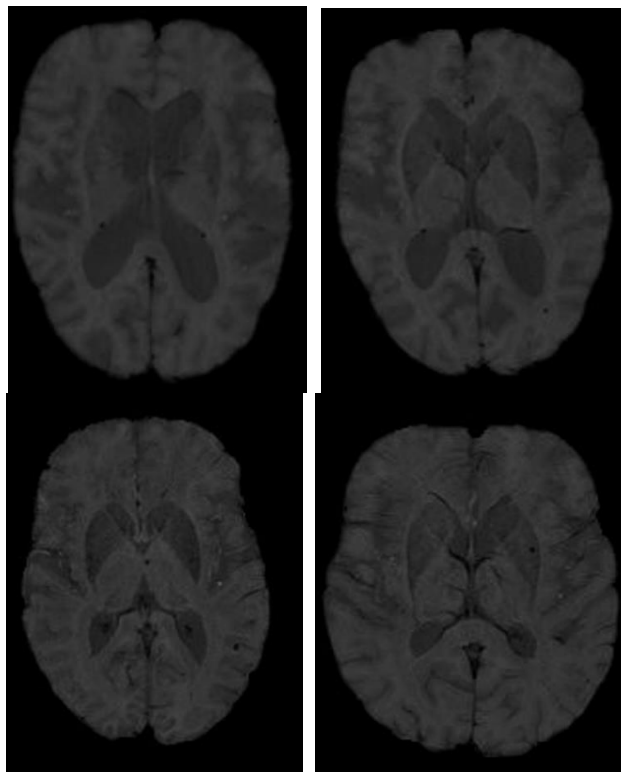


Fig. 3. Images from the database used for cerebral microbleeds.

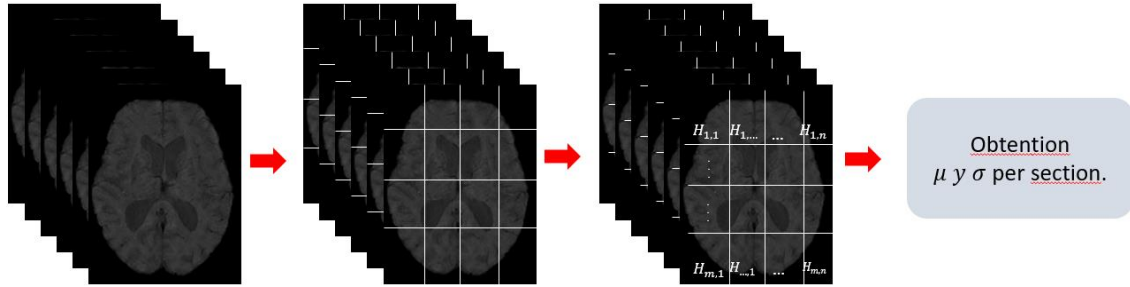


Fig. 4. Diagram outlining Phase I.

Shannon entropy was implemented to assess the complexity of information in each image segment. This analysis was applied to the 50 images, obtaining entropies for each section in each image. Then, the mean and standard deviation of the entropies were calculated, providing a detailed insight into the variability in images of patients without microbleeds. In the second phase, images of patients with recorded microbleeds, part of a database of 57 images of non-healthy patients, were introduced. These images were processed similarly, dividing them into 16 sections and evaluating them in terms of entropy, as shown in Fig. 5. The Z-score was applied to quantify the standard deviations of entropy with respect to the mean of images from healthy patients, allowing for an accurate assessment of variations in image complexity.

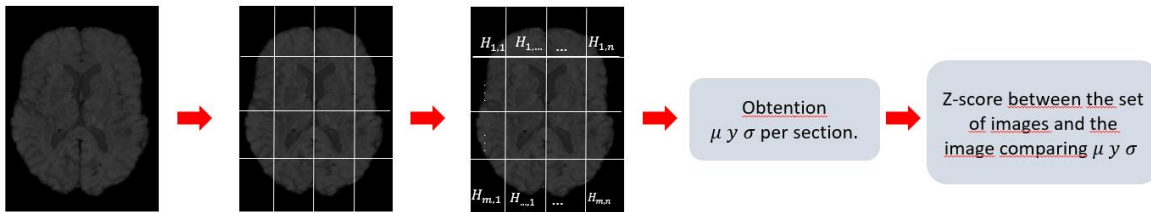


Fig. 5. Diagram outlining Phase II.

The validation of the results involved a comparison using a different segmentation with 32 sections of different geometries. The similarity in entropy values confirmed the robustness of the results.

3 Results and Discussion

The results were obtained using a specific algorithm developed for this task, utilizing Anaconda Navigator and Spyder 5.4.3 on a laptop computer (LENOVO) 82FG with an 11th Gen Intel(R) Core(TM) i5-1135G7 @ 2.40GHz processor, 2419 Mhz, 4 main processors, and 8 logical processors. The code used mainly consists of parameters for Shannon entropy, Z-score, and image type, which are essential to be grayscale images.

In Figure 6, the results corresponding to the images segmented into 16 and 32 sections, respectively, are presented.

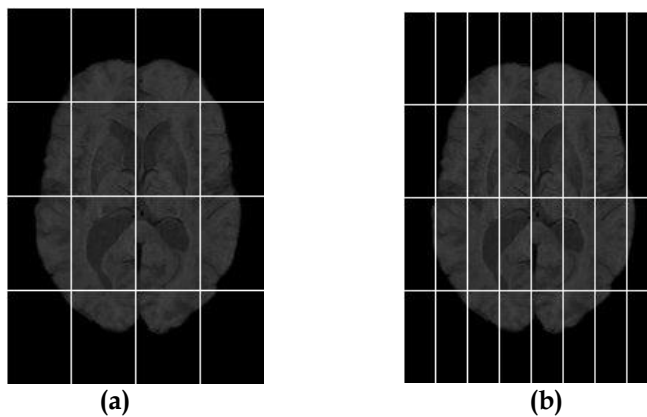


Fig. 6. Diagram outlining phase II (a) 16 sections, (b) 32 sections.

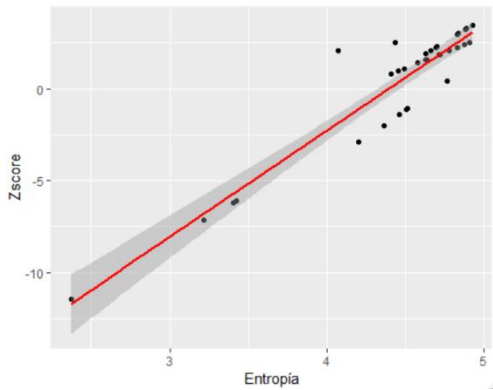
Below are some of the results obtained according to the selected images, along with their respective entropy values and their respective Z-scores.

Nombre	lugar	Val. entropia	Z-score
Imagen_SWI_1	5,2	4.82799	2.2668
Imagen_SWI_2	5,1	4.7796	2.1009
Imagen_SWI_3	4,2	4.8328	2.9898
Imagen_SWI_4	4,2	4.9238	3.4676
Imagen_SWI_5	5,2	4.4115	0.83694
Imagen_SWI_6	4,1	4.7019	2.3017
Imagen_SWI_7	6,2	4.5045	-1.137351
Imagen_SWI_8	4,1	4.6287	1.9172
Imagen_SWI_9	6,2	4.2002	-2.9019
Imagen_SWI_10	5,2	4.6359	1.6074
Imagen_SWI_11	7,1	2.3721	-11.44994
Imagen_SWI_12	7,1	3.4229	-6.0782
Imagen_SWI_13	5,1	4.7131	1.8724
Imagen_SWI_14	5,1	4.5785	1.4105
Imagen_SWI_15	5,1	4.4913	1.111
Imagen_SWI_16	3,2	4.4333	2.5445
Imagen_SWI_17	5,1	4.7171	1.8862
Imagen_SWI_18	4,1	4.834	2.9957
Imagen_SWI_19	5,2	4.9057	2.5336
Imagen_SWI_20	4,1	4.8821	3.2484
Imagen_SWI_23	4,2	4.4526	0.9922

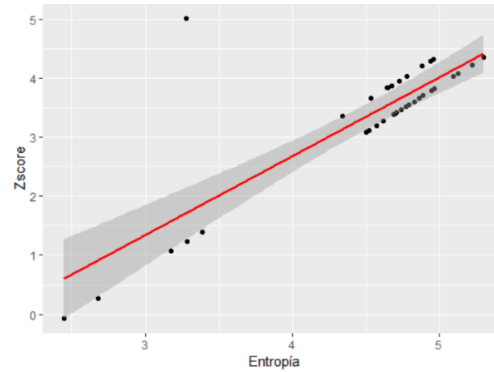
Table 1

Nombre	lugar	Val. entropia	Z-score
Imagen_SWI_1	2,5	4.7786	4.0422
Imagen_SWI_2	1,4	3.2745	5.0249
Imagen_SWI_3	3,6	4.9682	3.8291
Imagen_SWI_4	3,2	4.969	3.8304
Imagen_SWI_5	2,6	4.6459	3.8374
Imagen_SWI_7	2,4	4.8862	4.2082
Imagen_SWI_8	3,5	4.7432	3.4716
Imagen_SWI_9	2,2	4.9419	4.2942
Imagen_SWI_10	4,5	2.44587	-0.0658
Imagen_SWI_11	3,4	4.7957	3.555
Imagen_SWI_12	3,4	4.8292	3.6083
Imagen_SWI_13	3,6	4.5726	3.2002
Imagen_SWI_16	3,6	4.6918	3.3899
Imagen_SWI_17	3,3	4.7086	3.4164
Imagen_SWI_18	3,6	4.5709	3.1977
Imagen_SWI_19	3,6	4.5231	3.1216
Imagen_SWI_22	3,7	4.8651	3.6652
Imagen_SWI_23	3,5	5.2234	4.2348

Table 2



Graph 1



Graph 2

3.1 Statical Analysis

A Pearson correlation analysis was conducted between entropy and Z-score values, providing a deeper understanding of the relationship between these parameters. The similarity in entropy values confirmed the robustness of the results obtained. Two scatterplots with regression lines were analyzed, representing entropy data along with their respective Z-score values, revealing correlations of 0.9418 and 0.8295, respectively.

In the context of statistical analysis, the scarcity of entropy samples prompted the application of a Student's t-test for two independent samples. The purpose was to verify if the means were equal in order to combine both samples and obtain a larger sample.

The result of the t-test yielded a p-value of 0.6516, which exceeds a common significance level of 0.05. This finding indicates that there is not enough evidence to reject the null hypothesis. Consequently, no significant difference has been found between the means of the two samples.

Using the larger sample, a standard error of the mean of 0.096 was determined. This allowed us to establish a confidence interval of 4.3362 to 4.6042 for the mean entropy of microbleeds, with a margin of error of 1.79%.

Furthermore, an interval describing the possible presence of microbleeds through entropy was identified, located within a range of one standard deviation from 3.8174 to 5.123.

3.2 Discussions

The present study provides a quantitative representation of cerebral microbleeds through the measurement of their entropy. The results obtained are presented in Tables 1 and 2, which show the values corresponding to the sections where microbleeds were detected. To assess the disparity of these values with respect to the mean, the Z-score value is employed. The table shows the values of the sections containing at least one microbleed; in certain images, multiple microbleeds were identified, which were also recorded in the table. A correlation analysis between these variables is conducted using the Pearson coefficient. The results reveal a positive correlation between both variables, as illustrated in Figures 1 and 2, as expected since the obtained data are centered on the microbleed areas. Additionally, the correlation matrix yields values of 0.9417 and 0.8295 respectively. In future work, it is intended to verify with other databases whether there is replicability of these findings, thus confirming that these correlations persist.

A limitation for the Student's t-test was the small sample size. However, one of the assumptions to consider is the normality of the data, and since there were slightly more than 30 data points in each sample, the test could be conducted to demonstrate that both are statistically different from a mean of 4, as both cases have extremely small p-values. With these results, a larger sample could be obtained, which is considered a strategy as it does not affect the representativeness of the sample used and does not influence the interpretation of the obtained results. These results allowed us to determine a confidence interval in which we can say with 95% confidence that the true mean will lie between 4.3362 and 4.6042, with an error of 1.79%.

Furthermore, in the study, according to the obtained data, an interval was found that allows us to detect a possible cerebral microbleed through its entropy. This interval is described by means of a standard deviation of the data. This study is considered an important step towards the statistical quantification of a microbleed.

It is important to consider that this could be a significant step towards early detection of cerebral microbleeds for neurodegenerative diseases.

It is crucial to mention that one of the limitations of this study lies in the lack of a sufficiently extensive and preprocessed database to conduct a more thorough analysis. As future work, similar research is proposed, testing different databases but with previously processed images and an adequate amount of data, in order to optimize and improve the accuracy of our study. This work is considered a preliminary study in the automatic processing of images using convolutional neural networks.

4 Conclusions

This study achieves the quantitative detection of cerebral microbleeds through the statistical analysis of entropy, obtaining a range for potential microbleed detection. The values obtained provide valuable information that can significantly contribute to the early detection of these anomalies in the human brain. Despite being a preliminary work, its relevance is highlighted as it represents an important step towards the precise identification of microbleeds. This quantitative approach not only expands our understanding of these conditions but could also have a significant impact on the diagnosis and early treatment of patients with cerebral microbleeds. For future work, improving the code in terms of efficiency is expected, i.e., adding metrics to the study to enhance detection capability including time.

5 Acknowledgments

Acknowledgments to CSIRO for providing the database and to the Biomedical Informatics Group ResDevCons under the supervision of Jurgen Mejan-Fripp by CSIRO (Australia).

References

[1] Y. Zou, J. Zhang, M. Upadhyay, S. Sun and T. Jiang, "Automatic Image Thresholding Based on Shannon Entropy Difference and Dynamic Synergic Entropy," in *IEEE Access*, vol. 8, pp. 171218-171239, 2020, doi: 10.1109/ACCESS.2020.3024718. keywords:

- {Entropy;Histograms;Image segmentation;Thresholding (Imaging);Image edge detection;Correlation;Automatic thresholding;principle of maximum entropy;Shannon entropy difference;dynamic synergic entropy},
- [2] Greenberg, S.M., Vernooij, M.W., Cordonnier, C., Viswanathan, A., Salman, R.A.S., Warach, S., Launer, L.J., Van Buchem, M.A. and Breteler, M.M., 2009. Cerebral microbleeds: a guide to detection and interpretation. *The Lancet Neurology*, 8(2), pp.165-174.
- [3] Ayaz, M., Boikov, A.S., Haacke, E.M., Kido, D.K. and Kirsch, W.M., 2010. Imaging cerebral microbleeds using susceptibility weighted imaging: one step toward detecting vascular dementia. *Journal of Magnetic Resonance Imaging*, 31(1), pp.142-148.
- [4] Haacke, E.M., Mittal, S., Wu, Z., Neelavalli, J. and Cheng, Y.C., 2009. Susceptibility-weighted imaging: technical aspects and clinical applications, part 1. *American Journal of Neuroradiology*, 30(1), pp.19-30.
- [5] Park, J.H., Park, S.W., Kang, S.H., Nam, T.K., Min, B.K. and Hwang, S.N., 2009. Detection of traumatic cerebral microbleeds by susceptibility-weighted image of MRI. *Journal of Korean Neurosurgical Society*, 46(4), p.365.
- [6] Nandigam, R.N.K., Viswanathan, A., Delgado, P., Skehan, M.E., Smith, E.E., Rosand, J., Greenberg, S.M. and Dickerson, B.C., 2009. MR imaging detection of cerebral microbleeds: effect of susceptibility-weighted imaging, section thickness, and field strength. *American Journal of Neuroradiology*, 30(2), pp.338-343.
- [7] Koschmieder, K., Paul, M. M., van den Heuvel, T. L. A., van der Eerden, A. W., van Ginneken, B., & Manniesing, R. (2022). Automated detection of cerebral microbleeds via segmentation in susceptibility-weighted images of patients with traumatic brain injury. *NeuroImage: Clinical*, 35, 103027.
- [8] Buch, S., Cheng, Y.C.N., Hu, J., Liu, S., Beaver, J., Rajagovindan, R. and Haacke, E.M., 2017. Determination of detection sensitivity for cerebral microbleeds using susceptibility-weighted imaging. *NMR in biomedicine*, 30(4), p.e3551.
- [9] Liu, S., Utriainen, D., Chai, C., Chen, Y., Wang, L., Sethi, S.K., Xia, S. and Haacke, E.M., 2019. Cerebral microbleed detection using susceptibility weighted imaging and deep learning. *Neuroimage*, 198, pp.271-282.
- [10] Al-Masni, M.A., Kim, W.R., Kim, E.Y., Noh, Y. and Kim, D.H., 2020. Automated detection of cerebral microbleeds in MR images: A two-stage deep learning approach. *NeuroImage: Clinical*, 28, p.102464.
- [11] Ateeq, T., Faheem, Z.B., Ghoneimy, M., Li, Y. and Baz, A., 2023. Naïve bayes classifier assisted automated detection of cerebral microbleeds in SWI brain images.
- [12] Van den Heuvel, T. L. A., Van Der Eerden, A. W., Manniesing, R., Ghafoorian, M., Tan, T., Andriessen, T. M. J. C., ... & Platel, B. (2016). Automated detection of cerebral microbleeds in patients with traumatic brain injury. *NeuroImage: Clinical*, 12, 241-251.
- [13] Hong, J., Wang, S. H., Cheng, H., & Liu, J. (2020). Classification of cerebral microbleeds based on fully-optimized convolutional neural network. *Multimedia Tools and Applications*, 79, 15151-15169.
- [14] Liu, S., Utriainen, D., Chai, C., Chen, Y., Wang, L., Sethi, S. K., ... & Haacke, E. M. (2019). Cerebral microbleed detection using susceptibility weighted imaging and deep learning. *Neuroimage*, 198, 271-282.
- [15] Barnes, S. R., Haacke, E. M., Ayaz, M., Boikov, A. S., Kirsch, W., & Kido, D. (2011). Semiautomated detection of cerebral microbleeds in magnetic resonance images. *Magnetic resonance imaging*, 29(6), 844-852
- [16] Mello Román, Julio César, José Luis Vázquez Noguera, Horacio Legal-Ayala, Diego P. Pinto-Roa, Santiago Gomez-Guerrero, and Miguel García Torres. 2019. "Entropy and Contrast Enhancement of Infrared Thermal Images Using the Multiscale Top-Hat Transform" *Entropy* 21, no. 3: 244. <https://doi.org/10.3390/e21030244>
- [17] Zou, Y., Zhang, J., Upadhyay, M., Sun, S., & Jiang, T. (2020). Automatic image thresholding based on Shannon entropy difference and dynamic synergic entropy. *Ieee Access*, 8, 171218-171239.
- [18] Naidu, M. S. R., Kumar, P. R., & Chiranjeevi, K. (2018). Shannon and fuzzy entropy based evolutionary image thresholding for image segmentation. *Alexandria engineering journal*, 57(3), 1643-1655.
- [19] El-Sayed, M. A., & Hafeez, T. A. E. (2012). New edge detection technique based on the shannon entropy in gray level images. *arXiv preprint arXiv:1211.2502*.
- [20] Sadek, S., & Abdel-Khalek, S. (2013). Generalized α -entropy based medical image segmentation. *Journal of Software Engineering and Applications*, 2014.
- [21] Pandey, V., & Gupta, V. (2014). MRI image segmentation using Shannon and non Shannon entropy measures. *International Journal of Application or Innovation in Engineering & Management*, 3(7), 41-46.
- [22] Sen, H., & Agarwal, A. (2015). Shannon and Non Shannon Entropy Based MRI Image Segmentation. *International Bulletin of Mathematical Research*, 2(1), 290-296.
- [23] Ghosh, M., Das, D., & Chakraborty, C. (2010, December). Entropy based divergence for leukocyte image segmentation. In *2010 International Conference on Systems in Medicine and Biology* (pp. 409-413). IEEE.
- [24] Pharwaha, A. P. S., & Singh, B. (2009, October). Shannon and non-shannon measures of entropy for statistical texture feature extraction in digitized mammograms. In *Proceedings of the world congress on engineering and computer science* (Vol. 2, pp. 20-22).
- [25] Wu, Y., Zhou, Y., Saveriades, G., Agaian, S., Noonan, J. P., & Natarajan, P. (2013). Local Shannon entropy measure with statistical tests for image randomness. *Information Sciences*, 222, 323-342.
- [26] Paul, S., & Bandyopadhyay, B. (2014, February). A novel approach for image compression based on multi-level image thresholding using Shannon entropy and differential evolution. In *Proceedings of the 2014 IEEE Students' Technology Symposium* (pp. 56-61). IEEE.
- [27] Gull, S. F., & Skilling, J. (1984, October). Maximum entropy method in image processing. In *Iee proceedings f (communications, radar and signal processing)* (Vol. 131, No. 6, pp. 646-659). IET Digital Library.
- [28] Momeni, Saba; Fazlollahi, Amir; Yates, Paul; Christopher, Rowe; Gao, Yongsheng; Wee-Chung Liew, Alan; Salvado, Olivier (2021): Synthetic Cerebral Microbleed on SWI images. v1. CSIRO. Data Collection. <https://doi.org/10.25919/aegy-ny12>
- [29] Cover, T. M., & Thomas, J. A. (2006). *Elements of Information Theory* (2nd ed.). Wiley-Interscience
- [30] MacKay, D. J. C. (2003). *Information Theory, Inference, and Learning Algorithms*. Cambridge University Press.

- [31] Li, C., & Deng, X. (2014). Entropy-Based Adaptive Image Segmentation Using Improved Genetic Algorithm. *Entropy*, 16(6), 3276-3293. [DOI: 10.3390/e16063276]
- [32] Mahdianpari, M., & Rezaeian, A. (2017). Medical Image Fusion Using Wavelet Transform and Shannon Entropy. *Signal, Image and Video Processing*, 11(1), 57-64. [DOI: 10.1007/s11760-016-0897-4]
- [33] He, X., & Yang, J. (2014). An Adaptive Edge-Based Image Steganography Using LSB Matching Revisited and Modulus Function with Entropy. *Mathematical Problems in Engineering*, 2014, 1-11. [DOI: 10.1155/2014/413178]
- [34] Chen, Y., & Zhang, Y. (2014). Application of Shannon Wavelet Entropy in Image Fusion. *International Journal of Distributed Sensor Networks*, 10(7), 756538. [DOI: 10.1155/2014/756538]

Dataset:

- [1] Haacke, E. M., & Reichenbach, J. R. (Eds.). (2011). *Susceptibility weighted imaging in MRI: Basic concepts and clinical applications* (p. 203). Hoboken, New Jersey: Wiley-Blackwell.